Research Article

Dumitru Baleanu, Sania Qureshi*, Amanullah Soomro, and Asif Ali Shaikh

Variable stepsize construction of a two-step optimized hybrid block method with relative stability

Abstract: Several numerical techniques for solving initial value problems arise in physical and natural sciences. In many cases, these problems require numerical treatment to achieve the required solution. However, in today's modern era, numerical algorithms must be cost-effective with suitable convergence and stability features. At least the fifth-order convergent two-step optimized hybrid block method recently proposed in the literature is formulated in this research work with its variable stepsize approach for numerically solving first- and higher-order initial-value problems in ordinary differential equations. It has been constructed using a continuous approximation achieved through interpolation and collocation techniques at two intra-step points chosen by optimizing the local truncation errors of the main formulae. The theoretical analysis, including order stars for the relative stability, is considered. Both fixed and variable stepsize approaches are presented to observe the superiority of the latter approach. When tested on challenging differential systems, the method gives better accuracy, as revealed by the efficiency plots and the error distribution tables, including the machine time measured in seconds.

Keywords: stiff models, adaptive stepsize, A-stability, optimal intra-step points, order stars

* **Corresponding author: Sania Qureshi,** Department of Basic Sciences and Related Studies, Mehran University of Engineering and Technology, Jamshoro – 76062, Pakistan; Department of Mathematics, Near East University TRNC, Mersin 10, Turkey, e-mail: sania.qureshi@faculty.muet.edu.pk
Dumitru Baleanu: Department of Mathematics, Faculty of Arts and Sciences, Cankaya University, 06530, Ankara, Turkey; Institute of Space Sciences, P.O. Box, MG-23, R 76900, Magurele-Bucharest, Romania; Department of Medical Research, China Medical University Hospital, China Medical University, Taichung, Taiwan
Amanullah Soomro, Asif Ali Shaikh: Department of Basic Sciences and Related Studies, Mehran University of Engineering and Technology, Jamshoro – 76062, Pakistan

1 Introduction

The initial value problems of the following form are the most frequently used problems in several fields of studies:

$$w'(x) = g(x, w(x)); \quad w(x_0) = w_0, \tag{1}$$

where $x \in [a, b] \subset \mathbb{R}$ and $w(x), g(x, w(x)) \in \mathbb{R}^n$. The assumption on the existence of a unique continuously differentiable solution $w(x)$ under suitable conditions is made. The assumption confirms that problem (1) is well-posed. In every discipline of science, the aforementioned type of equations often arise. Several models relying on ordinary differential equations have been suggested to understand the dynamic behavior of the coronavirus pandemic, shown in refs [1–3], reaction-rate equations [4], exponential growth/decay [5], van der Pol oscillator [6], nonlinear corneal shape model [7], electrical, hydraulic and mechanical systems with variable mass [8], double pendulum [9], logistic growth [10], and many more.

The non-linearity and stiffness of some models make it more difficult for applied mathematicians to devise efficient ways of obtaining approximate solutions with sufficient accuracy in a short amount of time. Various numerical methods, such as explicit and implicit Runge–Kutta (RK)-type methods, diagonally implicit RK methods, singly diagonally implicit RK methods, linear multistep methods, including Adams–Bashforth/Moulton methods, backward and forward differential methods, multi-derivative methods, rational/nonlinear methods, trigonometrically fitted methods, and hybrid block methods, have been created in the past and recent literature in search of better accuracy and time-efficiency. The block techniques have been prevalent among the scientific community due to their self-starting characteristics and ability to avoid overlapping piece-wise solutions. These methods, which include both primary and supplemental procedures, can be used to obtain an approximate solution at multiple intra-step points at the same time, as shown in refs [11–14].

Several optimal block techniques have recently been developed in the literature to solve first and higher order ordinary differential equations, including one-, two-, four-, five-, six-, and seven-step block techniques. Nonetheless, only a small fraction of these approaches are considered for practical purposes owing to their limitations on the accuracy and convergence features. Therefore, we have been motivated to devise some strategies for the block methods to reduce functional evaluations (FEs) and computational costs. This is achieved in the present work by the formulation of an adaptive version of a block method available in the literature. As long as the block methods are concerned, there are many applications wherein these methods are helpful. For example, the nonlinear logistic growth model is often used in population dynamics, the mass spring damper system in physics, resistor-inductor-capacitor series circuits in electronics, the Prothero–Robinson problem in chemistry, the periodic orbit system in quantum mechanics, and many other fields.

We try to formulate a variable stepsize version of the two-step optimal block method (OBM) with reasonably regular use and growing preference for efficient and robust block methods. It may be noted that the constant stepsize version is also reformulated here for a quick reference. Although several researchers have recently developed some of the optimized block techniques [15–17], they are either computationally expensive, have a lower order of convergence, or are only suitable for a specific class of initial value problems. In addition, most of them have not been represented in their RK form and reformulation versions. The unique feature related to the reformulated version of a block method was first proposed by Ramos in ref. [18] whose algorithm is being employed herein for the variable stepsize formulation and discussing its relative stability. The improvement of the method considering the variable step size implementation in the present research work is an advance in the performance of the strategy as adopted in ref. [19].

The present study is designed as follows: Section 2 contains the derivation of the optimized two-step hybrid block method with two intra-step points, where the optimization strategy is explained in-depth, as well as the reformulation of the method, including its implicit RK structure. Sections 3 and 4 include the order stars (relative stability) and variable stepsize approach, respectively. In Section 5, various challenging nonlinear stiff models from different fields of engineering and science are considered, where numerical results are achieved using both constant and variable stepsize approaches of the two-step optimized hybrid block method and some existing methods with similar properties. Finally, Section 6

concludes the research findings with some recommendations for future study.

2 Derivation of the optimized block method

In this section, we derive the two-step optimized block technique with two intra-step points, where both intra-step points are optimized from the local truncation error (LTE) of the main formula. Let us consider the partition $a = x_0 < x_1 < x_2, \cdots < x_N = b$ on the integration interval $[a, b]$ with stepsize $\Delta x = x_{k+1} - x_k$, $k = 0, 1, 2, \ldots, N - 1$, and assume that on a generic sub-interval $[x_n, x_{n+2}]$, the true solution $w(x)$ of (1) can be approximated by a polynomial $Q(x)$ in the following form:

$$w(x) \approx Q(x) = \sum_{j=0}^{5} \delta_j x^j, \tag{2}$$

where $\delta_j \in \mathbb{R}$ represent real unknown parameters. When Eq. (2) is differentiated, the following result is obtained:

$$w'(x) \approx Q'(x) = \sum_{j=1}^{5} j\delta_j x^{j-1}. \tag{3}$$

Consider two intra-step points, $x_{n+r} = x_n + r\Delta x$, $x_{n+s} = x_n + s\Delta x$ with $0 < r < 1 < s < 2$, to compute the approximate solution of the initial value problem (IVP) (1) at the point x_{n+2}, assuming that $w_n = w(x_n)$. To start the procedure, consider the approximation in (2) determined at x_n, and its first-order derivative determined at the points $x_n, x_{n+r}, x_{n+1}, x_{n+s}, x_{n+2}$. By so doing, we obtain the following linear system of six equations in six real unknown parameters δ_j, $j = 0, 1, \ldots 5$:

$$\begin{pmatrix} 1 & x_n & x_n^2 & x_n^3 & x_n^4 & x_n^5 \\ 0 & 1 & 2x_n & 3x_n^2 & 4x_n^3 & 5x_n^4 \\ 0 & 1 & 2x_{n+r} & 3x_{n+r}^2 & 4x_{n+r}^3 & 5x_{n+r}^4 \\ 0 & 1 & 2x_{n+1} & 3x_{n+1}^2 & 4x_{n+1}^3 & 5x_{n+1}^4 \\ 0 & 1 & 2x_{n+s} & 3x_{n+s}^2 & 4x_{n+s}^3 & 5x_{n+s}^4 \\ 0 & 1 & 2x_{n+2} & 3x_{n+2}^2 & 4x_{n+2}^3 & 5x_{n+2}^4 \end{pmatrix} \begin{pmatrix} \delta_0 \\ \delta_1 \\ \delta_2 \\ \delta_3 \\ \delta_4 \\ \delta_5 \end{pmatrix} = \begin{pmatrix} w_n \\ g_n \\ g_{n+r} \\ g_{n+1} \\ g_{n+s} \\ g_{n+2} \end{pmatrix}. \tag{4}$$

Solution of the above linear system gives values of the six unknown parameters that are not shown here for brevity. These parameters will determine the coefficients of the polynomial $Q(x)$ in terms of $w_n, g_n, g_{n+r}, g_{n+1}, g_{n+s}$, and g_{n+2}. Putting these values in (2) while using the change of variable $x = x_n + t\Delta x$, we reach the following:

$$Q(t) = \delta_0 w_n + (\eta_0 g_n + \eta_r g_{n+r} + \eta_1 g_{n+1} + \eta_s g_{n+s} + \eta_2 g_{n+2}), \tag{5}$$

where

$$\delta_0 = 1,$$

$$\eta_0 = \Delta x \frac{(20rst^2 - 15rt^3 - 15st^3 + 12t^4 - 90rst + 60rt^2 + 60st^2 - 45t^3 + 120rs - 60rt - 60st + 40t^2)}{120rs},$$

$$\eta_r = -\frac{\Delta x t^2 (15st^2 - 12t^3 - 60st + 45t^2 + 60s - 40t)}{(60r - 60)(r - 2)(r - s)r},$$

$$\eta_1 = -\frac{\Delta x t^2 (20rst - 15rt^2 - 15st^2 + 12t^3 - 60s + 40rt + 40st - 30t^2)}{(60s - 60)(r - 1)},$$

$$\eta_s = \frac{\Delta x t^2 (15rt^2 - 12t^3 - 60rt + 45t^2 + 60r - 40t)}{(60s - 60)(s - 2)(r - s)s},$$

$$\eta_2 = \frac{\Delta x t^2 (20rst - 15rt^2 - 15st^2 + 12t^3 - 30rs + 20rt + 20st - 15t^2)}{(120s - 240)(r - 2)}.$$

To obtain the two-step block method, we evaluate $Q(t)$ at the collocation points x_{n+r}, x_{n+1}, x_{n+s}, and x_{n+2}, that is, we take $t = r, 1, s, 2$. This results in the following formulas that can be considered as a hybrid block method with two parameters:

$$w_{n+r} = w_n + \frac{g_n \Delta x (-3r^4 + 5r^3 s + 15r^3 - 30r^2 s - 20r^2 + 60rs)}{120s} - \frac{g_{n+r} \Delta x r (-12r^3 + 15r^2 s + 45r^2 - 60rs - 40r + 60s)}{(60r - 60)(r - 2)(r - s)}$$
$$+ \frac{g_{n+1} \Delta x r^2 (-3r^3 + 5r^2 s + 10r^2 - 20rs)}{(60s - 60)(r - 1)} - \frac{g_{n+s} \Delta x r^2 (3r^3 - 15r^2 + 20r)}{(60s - 60)(s - 2)(r - s)s} + \frac{g_{n+2} \Delta x r^2 (-3r^3 + 5r^2 s + 5r^2 - 10rs)}{(120s - 240)(r - 2)}, \quad (6)$$

$$w_{n+1} = w_n + \frac{g_n \Delta x (50rs - 15r - 15s + 7)}{120rs} - \frac{g_{n+r} \Delta x (15s - 7)}{(60r - 60)(r - 2)(r - s)r} - \frac{g_{n+1} \Delta x (-40rs + 25r + 25s - 18)}{(60s - 60)(r - 1)}$$
$$+ \frac{g_{n+s} \Delta x (15r - 7)}{(60s - 60)(s - 2)(r - s)s} + \frac{g_{n+2} \Delta x (-10rs + 5r + 5s - 3)}{(120s - 240)(r - 2)}, \quad (7)$$

$$w_{n+s} = w_n + \frac{g_n \Delta x (5rs^3 - 3s^4 - 30rs^2 + 15s^3 + 60rs - 20s^2)}{120r} + - \frac{g_{n+r} \Delta x s^2 (3s^3 - 15s^2 + 20s)}{(60r - 60)(r - 2)(r - s)r}$$
$$- \frac{g_{n+1} \Delta x s^2 (5rs^2 - 3s^3 - 20rs + 10s^2)}{(60s - 60)(r - 1)} + \frac{g_{n+s} \Delta x s (15rs^2 - 12s^3 - 60rs + 45s^2 + 60r - 40s)}{(60s - 60)(s - 2)(r - s)}$$
$$+ \frac{g_{n+2} \Delta x s^2 (5rs^2 - 3s^3 - 10rs + 5s^2)}{(120s - 240)(r - 2)}, \quad (8)$$

$$w_{n+2} = w_n + \frac{g_n \Delta x (20rs - 8)}{60rs} - \frac{4g_{n+r} \Delta x}{(15r - 15)(r - 2)(r - s)r} - \frac{1}{15} \frac{g_{n+1} \Delta x (-20rs + 20r + 20s - 24)}{(s - 1)(r - 1)}$$
$$+ \frac{4g_{n+s} \Delta x}{(15s - 15)(s - 2)(r - s)s} + \frac{1}{30} \frac{g_{n+2} \Delta x (10rs - 20r - 20s + 36)}{(s - 2)(r - 2)}, \quad (9)$$

where $w_{n+i} \simeq w(x_n + i\Delta x)$ are approximations of the true solution, and $g_{n+i} = g(x_{n+i}, w_{n+i})$, for $i = r, 1, s, 2$. Two unknown parameters r, s are related to the intra-step points x_r, x_s in the above-obtained approximations. We will equate the first leading term of the LTE of w_{n+1} and w_{n+2} to zero to achieve appropriate values for these parameters. As a result, optimal values for the parameters will be obtained, and at the end of the sub-interval $[x_n, x_{n+2}]$, the value w_{n+2} will be the only value required to forward the integration to the next sub-interval. As a result, we consider the LTE of the formula given in (9) as:

$$\mathcal{L}(w(x_{n+1}); \Delta x) = \frac{((15s - 7)r - 7s + 4)w^{(6)}(x_n)(\Delta x)^6}{7200}$$
$$+ \frac{(7r^2(15s - 7) + 7r(15s^2 + 38s - 21) - 49s^2 - 147s + 102)w^{(7)}(x_n)(\Delta x)^7}{302,400} + O(\Delta x)^8. \quad (10)$$

$$\mathcal{L}(w(x_{n+2}); \Delta x) = \frac{1}{450}(r + s - 2)w^{(6)}(x_n)(\Delta x)^6 + \frac{(7r^2 + 7r(s + 3) + 7s^2 + 21s - 66)w^{(7)}(x_n)(\Delta x)^7}{18,900} + O(\Delta x)^8. \quad (11)$$

At this stage, there are two parameters (r and s). We find the values of these two unknown parameters from leading terms of the LTEs as given in the aforementioned formulas for w_{n+1} and w_{n+2}. Therefrom, we obtain the following optimal values of the required parameters:

$$r = \frac{1}{3}(3 - \sqrt{3}), \quad s = \frac{1}{3}(3 + \sqrt{3}).$$

Substituting these values in (10) and (11), we obtain:

$$\mathcal{L}(w(x_{n+1}); \Delta x) = -\frac{(\Delta x)^7 w^{(7)}(x_n)}{56{,}700} + O(\Delta x^8),$$

$$\mathcal{L}(w(x_{n+2}); \Delta x) = -\frac{(\Delta x)^7 w^{(7)}(x_n)}{28{,}350} + O(\Delta x^8). \tag{12}$$

Thus, the two optimized parameters (intra-step points: r and s) yielded the following two-step optimized hybrid block method:

$$w_{n+r} = w_n + \Delta x\left(\frac{(29\sqrt{3} + 83)g_n}{180(\sqrt{3} + 3)} + \frac{(63\sqrt{3} + 171)g_{n+r}}{180(\sqrt{3} + 3)} + \frac{(-64\sqrt{3} + 32)g_{n+1}}{180(\sqrt{3} + 3)} + \frac{(-27\sqrt{3} + 81)g_{n+s}}{180(\sqrt{3} + 3)} + \frac{(-\sqrt{3} - 7)g_{n+2}}{180(\sqrt{3} + 3)}\right),$$

$$w_{n+1} = w_n + \Delta x\left(\frac{31g_n}{240} + \left(\frac{3}{16} + \frac{3\sqrt{3}}{10}\right)g_{n+r} + \frac{4g_{n+1}}{15} - \left(\frac{3}{16}\sqrt{3} + \frac{3}{10}\right)g_{n+s} + \frac{g_{n+2}}{240}\right),$$

$$w_{n+s} = w_n + \Delta x\left(\frac{(29\sqrt{3} - 83)g_n}{180(\sqrt{3} - 3)} + \frac{(-27\sqrt{3} - 81)g_{n+r}}{180(\sqrt{3} - 3)} + \frac{(-64\sqrt{3} - 32)g_{n+1}}{180(\sqrt{3} - 3)} + \frac{(63\sqrt{3} - 171)g_{n+s}}{180(\sqrt{3} - 3)} + \frac{(-\sqrt{3} + 7)g_{n+2}}{180(\sqrt{3} - 3)}\right),$$

$$w_{n+2} = w_n + \Delta x\left(\frac{2}{15}g_n + \frac{3}{5}g_{n+r} + \frac{8}{15}g_{n+1} + \frac{3}{5}g_{n+s} + \frac{2}{15}g_{n+2}\right). \tag{13}$$

It is worth to be noted that the above strategy concerning the optimization of the intra-step points was first introduced in ref. [20]. The pseudo-code for the above method is provided in Algorithm 1 under Appendix A. It is worth noting that the reformulation of the optimized block method produces substantial savings in the computational cost. The idea of reformulation is based on the strategy proposed by Ramos [18]. The reduction in the computational time comes from the fact that the number of FEs is reduced as follows:

$$\Delta x g_{n+r} = \left(\frac{-12 - \sqrt{3}}{6}w_n + \frac{3}{2}w_{n+r} + \frac{-4 + 4\sqrt{3}}{3}w_{n+1} + \frac{3 - 2\sqrt{3}}{3}w_{n+s} + \frac{2 - \sqrt{3}}{6}w_{n+2} - \frac{\Delta x}{3}g_n\right),$$

$$\Delta x g_{n+1} = \left(\frac{11}{8}w_n + \frac{-9 - 9\sqrt{3}}{8}w_{n+r} + w_{n+1} + \frac{-9 + 9\sqrt{3}}{8}w_{n+s} + \frac{1}{8}w_{n+2} + \frac{\Delta x}{4}g_n\right),$$

$$\Delta x g_{n+s} = \left(\frac{-12 + \sqrt{3}}{6}w_n + \frac{1}{4}(1 + \sqrt{3})(\sqrt{3} + 3)w_{n+r} + \frac{-4(1 + \sqrt{3})}{3}w_{n+1} + \frac{3}{2}w_{n+s} + \frac{1}{12}(1 + \sqrt{3})^2 w_{n+2} - \frac{\Delta x}{3}g_n\right),$$

$$\Delta x g_{n+2} = (5w_n - 9w_{n+r} + 8w_{n+1} - 9w_{n+s} + 5w_{n+2} + \Delta x g_n). \tag{14}$$

The above reformulation is later abbreviated as RBlock in the forthcoming sections. Moreover, the implicit RK structure of the optimized block method (13) is also presented through the usual Butcher tableau as follows:

0	0	0	0	0	0
$\frac{1}{2} - \frac{\sqrt{3}}{6}$	$\frac{83 + 29\sqrt{3}}{360(3 + \sqrt{3})}$	$\frac{171 + 63\sqrt{3}}{360(3 + \sqrt{3})}$	$\frac{32 - 64\sqrt{3}}{360(3 + \sqrt{3})}$	$\frac{81 - 27\sqrt{3}}{360(3 + \sqrt{3})}$	$\frac{-7 - \sqrt{3}}{360(3 + \sqrt{3})}$
$\frac{1}{2}$	$\frac{31}{480}$	$\frac{3}{20} + \frac{3\sqrt{3}}{32}$	$\frac{2}{15}$	$\frac{3}{20} - \frac{3\sqrt{3}}{32}$	$\frac{1}{480}$
$\frac{1}{2} + \frac{\sqrt{3}}{6}$	$\frac{83 - 29\sqrt{3}}{360(3 - \sqrt{3})}$	$\frac{81 + 27\sqrt{3}}{360(3 - \sqrt{3})}$	$\frac{32 + 64\sqrt{3}}{360(3 - \sqrt{3})}$	$\frac{171 - 63\sqrt{3}}{360(3 - \sqrt{3})}$	$\frac{-7 + \sqrt{3}}{360(3 - \sqrt{3})}$
1	$\frac{1}{15}$	$\frac{3}{10}$	$\frac{4}{15}$	$\frac{3}{10}$	$\frac{1}{15}$
1	$\frac{1}{15}$	$\frac{3}{10}$	$\frac{4}{15}$	$\frac{3}{10}$	$\frac{1}{15}$

In the section of numerical simulations, the abbreviation RKBlock is used for the method given in the above Butcher tableau.

3 Order stars

It has been commonly observed in the literature that the stability properties of various block methods generated through various techniques and steps are rarely investigated for their application to the theory of order stars (see refs [21,22]). Because there has been little discussion of this problem, we were motivated to perform a thorough analysis of the stability theory via order stars of the development of a new RK method and its economical implementation, which were taken into account in the current research work. These order stars play a crucial role in determining the relative stability of numerical techniques, as indicated by the order stars. Despite the fact that it may be used to examine regions of linear absolute stability of a $\mathcal{A}$-stable algorithm, the theory of order stars is a relatively new concept in the field of stability analysis. One of the fundamental publications in ref. [23] should be read in order to obtain a better understanding of the theoretical aspects of order stars that arise from the structure of numerical techniques such as those presented here. Consider two complex-valued polynomial type functions denoted by W_1 and W_2 having degree i and j, respectively, with the quotient denoted by $\Psi(\rho) = \frac{\rho_1}{\rho_2}$. As an example, consider the following stability function given in ref. [18] for the two-step optimized block method:

$$\Psi(\rho) = \frac{\rho^4 + 9\rho^3 + 39\rho^2 + 90\rho + 90}{\rho^4 - 9\rho^3 + 39\rho^2 - 90\rho + 90}. \quad (15)$$

The $\mathcal{A}$-stability characteristics have been depicted in Figure 1 for the method given in (13). The solution for the denominator ρ_2 in $\Psi(\rho)$ is called a pole. Another assumption is to consider a complex-valued function $\Omega(\rho)$ that plays a crucial role in rest of the analysis. An order star $\Phi(\rho)$ divides the complex plane $\mathbb{C}$ into three distinct areas which are shown as the triplet written as $\{T_+, T_0, T_-\}$. Members of the triplet can be defined in the following way:

$$
\begin{aligned}
T_+ &= \{\rho : \Phi(\rho) > c\}, \\
T_0 &= \{\rho : \Phi(\rho) = c\}, \\
T_- &= \{\rho : \Phi(\rho) < c\}.
\end{aligned} \quad (16)
$$

In available literature for the theory of order stars, two of its types are commonly used and referred to as the first and second type. Mathematically,
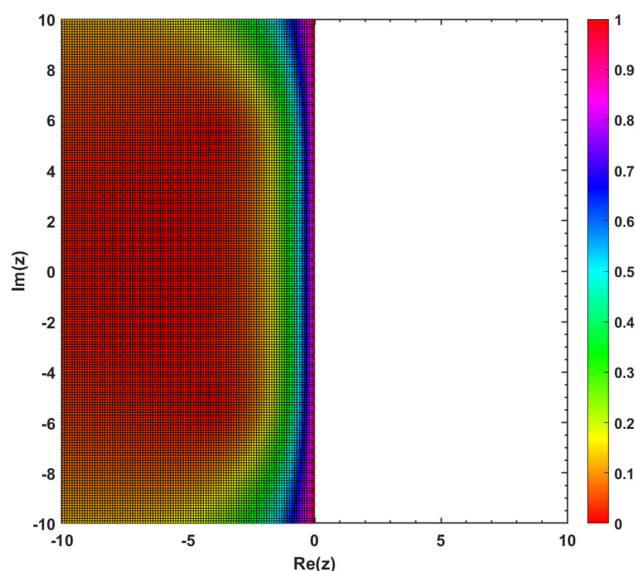

Figure 1: Region of absolute stability of the two-step optimized hybrid block method given in (13).

$$
\begin{aligned}
\Phi(\rho) &= \left| \frac{\Psi(\rho)}{\Omega(\rho)} \right| \quad \text{for } c - 1, \\
\Phi(\rho) &= \text{Re}(\Psi(\rho) - \Omega(\rho)) \quad \text{for } c = 0.
\end{aligned} \quad (17)
$$

There are always some distinguished features observed among the three triplets mentioned above. However, these features can be visualized graphically with the help of different shades given to their plotted regions. In this way, the region of growth of relative stability for the set R_+ is obvious and in the meantime contractivity region is shown by the triplet T_-. The triplet R_0 evidently represents the boundary for the remaining two triplets in $\mathbb{C}$. With the complex exponential function $\Omega(\rho) = \exp(\rho)$, our primary focus is upon the order stars of first kind. In this pursuit, the order star for the stability function $\Phi(\rho)$ given in (17) gives rise to the following three types of regions:

$$
\begin{aligned}
T_+ &= \{\rho \in \mathbb{C} : |\Psi(\rho)| > |\exp(-\rho)|\} \\
&= \{\rho \in \mathbb{C} : |\exp(-\rho)\Psi(\rho)| > 1\}, \\
T_0 &= \{\rho \in \mathbb{C} : |\Psi(\rho)| = |\exp(-\rho)|\} \\
&= \{\rho \in \mathbb{C} : |\exp(-\rho)\Psi(\rho)| = 1\}, \\
T_- &= \{\rho \in \mathbb{C} : |\Psi(\rho)| < |\exp(-\rho)|\} \\
&= \{\rho \in \mathbb{C} : |\exp(-\rho)\Psi(\rho)| < 1\}.
\end{aligned} \quad (18)
$$

When the above discussed regions are plotted in $\mathbb{C}$, the obvious star-like fingers became the reason for the shape to have name of order stars. An important concept related to the $\mathcal{A}$-acceptability has to be understood before we proceed with the said regions.

Definition 1. ($\mathcal{A}$-acceptability) The stability function $\Psi(\rho)$ is known as $\mathcal{A}$-acceptable if and only if T_+ does not come into contact with the imaginary line of the complex plane. In addition, $\Psi(\rho)$ must not have any poles in the region where $\mathrm{Re}(\rho) < 0$.

The plot of order stars for the optimized block method is shown in Figure 2, where the shaded regions depict the triplet T_+. It is worth noting that there is nothing common between T_+ and the imaginary axis. Additionally, no poles are seen in the left side of the complex plane, that is, where $\mathrm{Re}(\rho) < 0$. These essential characteristics show that the stability function of the optimized block method under investigation in the present research analysis has the properties of being $\mathcal{A}$-acceptable with $\mathrm{Re}(\rho) < 0$.

4 A variable stepsize formulation

With the help of an embedded-type procedure, this section discusses the formulation of the optimized block method (13) as a variable stepsize integrator. The procedure considers the combination of two methods of order α and order β with $\beta < \alpha$ and performs their simultaneous execution. The method (13) is taken as a higher order method with $\alpha = 5$, and we choose a lower order method with $\beta = 2$. The lower order method is used to obtain an approximation of the IVP (1) at the endpoint of the block $x = x_{n+1}$, denoted by w_{n+1}^*. This value is used to estimate the local error in w_{n+1}^* in comparison to the more accurate approximation w_{n+2}. The value w_{n+2} is used for advancing the integration process, called local extrapolation. The lower order formula is constructed to share the FEs with the method to control the computational cost. To

obtain a variable stepsize formulation, we used the following steps: Once the system in (13) has been solved, a new approximation of the solution is obtained with the lower order method at $x = x_{n+1}$, which is named as w_{n+1}^*. The corresponding local error le_{n+2} is

$$le_{n+2} = w(x_n + 2\Delta x) - w_{n+1}^*, \qquad (19)$$

where $w(x)$ shows the exact solution of the IVP in (1). For the solution w_{n+2} provided by the higher order method, we have $w(x_n + 2\Delta x) - w_{n+2} = O(\Delta x^{\alpha+1})$, and thus the local error estimation, EST, is obtained as

$$
\begin{aligned}
\mathrm{EST} &= w_{n+2} - w_{n+1}^*, \\
&= (w(x_n + 2\Delta x) - w_{n+1}^*) - (w(x_n + 2\Delta x) - w_{n+2}), \quad (20) \\
&= le_{n+2} + O(\Delta x^{\alpha+1}).
\end{aligned}
$$

This estimation corresponds to the local error of the lower order formula, since le_{n+2} is $O(\Delta x^{\beta+1})$ and hence dominates in (20) for enough small values of Δx as explained in ref. [24]. In the present study, we consider the following lower order formula called the implicit trapezoidal rule [25] with second-order convergence:

$$w^*(x_{n+1}) = w_n + \frac{\Delta x}{2}(g_n + g_{n+1}).$$

The aforementioned method is used because of the number of FEs to avoid any additional cost incurred by the lower order method. We have also used this second-order method for each method chosen in the present research work for the numerical simulations carried out under the variable stepsize approach. A local tolerance TOL is predefined during the implementation process by the user. If the estimated error EST is greater than tolerance (TOL), the algorithm automatically adjusts the step size from the previous value (Δx_{old}) to the new one (Δx_{new}), using the following formula:

$$\Delta x_{\mathrm{new}} = \kappa \Delta x_{\mathrm{old}} \left(\frac{\mathrm{TOL}}{\|\mathrm{EST}\|} \right)^{\frac{1}{\beta+1}}, \qquad (21)$$

where β represents the order of the lower order method and $0 < \kappa < 1$ is a safety factor whose purpose is to avoid failure steps. We assumed $\kappa = 0.95$ throughout the simulations for each method under consideration. In this process, the solver will keep trying until it obtains a stepsize for which the magnitude of EST is no more significant than the tolerance. Sometimes the solver might take much work to predict the new stepsize. To avoid this situation and prevent large fluctuations in the stepsizes, we impose some restrictions on the new stepsize (Δx_{new}), it is required to lie between Δx_{min} (minimum stepsize) and Δx_{max} (maximum stepsize), that is,

$$\Delta x_{\mathrm{min}} \leq \Delta x_{\mathrm{new}} \leq \Delta x_{\mathrm{max}}. \qquad (22)$$
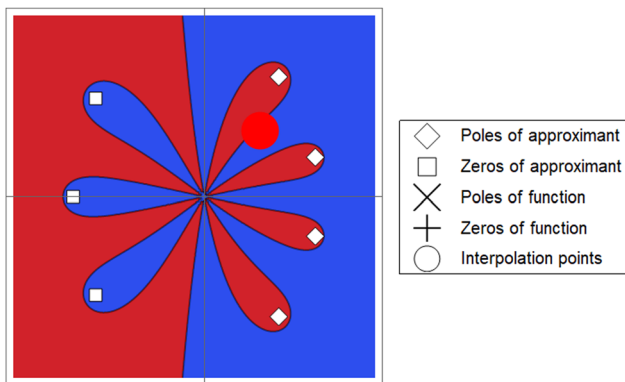

Figure 2: The plot of order stars for the two-step optimized hybrid block method given in (13).

On the other hand, when $||EST|| < TOL$, we can increase the step size for the next step, taking $\Delta x_{new} = c\Delta x_{old}$ with $c > 1$. Here, in the numerical experiments, we used $\Delta x_{new} = 2\Delta x_{old}$. A suitable initial stepsize (Δx_{ini}) is required to start the process, for which different approaches can be used (see ref. [26]). One of the most commonly used approaches is the one given in ref. [27], which is about selecting a small starting stepsize, and later the algorithm will fine-tune it according to the changing step size approach defined by the user. The pseudo-code for the variable stepsize version of the two-step optimized block method (13) is provided in Algorithm 2 under Appendix A.

5 Numerical dynamics with results and discussion

This section describes how the two-step optimized block method given in (13) performs while solving various types of mild and highly stiff application problems we come across in various fields from physical sciences. The method does not require several initial conditions or a predictor. While $n = 0$, the method (13) is solved as a system with $w(0) = w_0$ known to be the initial state of the system. After solving the problem at the initial state, we used the widely known second-order convergent Newton–Raphson method to obtain $w(x_1) = w_1$. The value $w(x_2) = w_2$ is then calculated using w_1 from the preceding block as the initial value, and the procedure is repeated until the last value at x_M is reached. We choose the duration of the integration interval as a multiple of $2\Delta x$ (i.e., $x_M - x_0 = k(2\Delta x)$, $k \in \mathbb{N}$) because the approach under consideration is two-step. The Newton–Raphson approach has been implemented using the Find Root command from Mathematica 12.1. It may be noted that all numerical computations are performed in Mathematica 12.1 on a personal computer running on Windows OS with Intel(R) Core(TM) i7-1065G7 CPU @ 1.30 GHz 1.50 GHz processor having 24.0 GB installed RAM. For comparison of the numerical simulations, we used three at least fifth-order methods, and one is the LobattoIIIA method of sixth-order. Five numerical experiments are presented, with two being scalar, while the other three are two- and four-dimensional systems. Considering the potentiality of block methods to deal with stiff differential models, we have taken some well-known stiff applied problems that have appeared several times in recent literature. These problems are solved with the following methods:

- Two-step at least fifth-order OBM (Block) with two intra-step points as given in (13).

- Two-step at least fifth-order OBM in reformulated version (RBlock) with two intra-step points.
- Two-step sixth-order OBM in RK form (RKBlock) with two intra-step points.
- One-step at least fifth-order OBM appeared in ref. [17].
- Laguerre polynomial hybrid block method (LPHBM) of at least fifth-order appeared in ref. [28].
- Fully-implicit RK-type fifth-order method called (Radau-I) appeared in [29, p. 226].
- Implicit RK-type sixth-order Lobatto method (Lob-III A) appeared in ref. [29, p. 228].

The performance of each method under consideration is measured on different types of errors including maximum global absolute errors $\max_{x \in [0, X_N]}||w(x_N) - w_N||_\infty$, absolute error at final grid point ($|w(x_N) - w_N|$), average absolute error $\frac{1}{N}(\sum_{i=1}^{N}|w(x_i) - w_i|)$, norm $(\sqrt{\sum_{i=1}^{N}|w(x_i) - x_i|^2})$, root mean square error $\left(\sqrt{\frac{\sum_{i=1}^{N}|w(x_i) - x_i|^2}{N}}\right)$, number of FEs, and the CPU time computed in seconds demonstrated by the efficiency curves. For numerical computations, both fixed and variable stepsize approaches are used for the first numerical experiment while only variable stepsize approach is employed for rest of the models under consideration.

Problem 1. We consider the following stiff system of first-order ODEs taken from ref. [30]:

$$
\begin{aligned}
w_1'(x) &= -w_1(x) + 95w_2(x), & w_1(0) &= 1, \\
w_2'(x) &= -w_1(x) - 97w_2(x), & w_2(0) &= 1,
\end{aligned}
\tag{23}
$$

where $x \in [0, 1]$. The exact solution of the aforementioned system is

$$
\begin{aligned}
w_1(x) &= \frac{1}{47}[95\exp(-2x) - 48\exp(-96x)], \\
w_2(x) &= \frac{1}{47}[48\exp(-96x) - \exp(-2x)].
\end{aligned}
\tag{24}
$$

In Problem 1, a two-dimensional system of ODEs is simulated with both fixed and variable stepsize approaches of the two-step optimized block method (13). In Table 1, the tolerance (ε) is set to 10^{-3} while the initial stepsize (Δx_{ini}) is assumed to be 10^{-1}. The number of steps (N) and the number of FEs are identical in both approaches for a fair comparison. The numerical errors, including norm, root mean square, and the arithmetic mean, are considerably smaller in the variable stepsize approach than the approach taken with a fixed step size. This comparison confirms the usefulness of the variable stepsize approach for the block method. It may also be noted that the superiority of the

Table 1: Comparison of errors with both fixed and variable stepsize approaches for Problem 1, with $\Delta x_{ini} = 10^{-1}$ and $\varepsilon = 10^{-3}$ via two-step optimized block method in (13)

N	FE	Approach	Norm$_\infty$	RMS	Mean
25	125	Fixed	9.672×10^{-4}	9.672×10^{-4}	9.672×10^{-4}
25	125	Variable	1.578×10^{-10}	1.116×10^{-10}	7.975×10^{-11}

latter approach is further confirmed in Table 2 when the tolerance is set to 10^{-6}. Moreover, since the variable stepsize approach is the major focus of this research investigation, numerical results are presented in the forthcoming simulations only with the variable stepsize approach for the two-step optimized block method given in (13), its reformulated version given in (14), and for its RK form as given by the Butcher tableau.

Problem 2. Consider another two-dimensional stiff problem [31]:

$$w_1'(x) = \mu w_1(x) + w_2^2(x), \quad w_1(0) = -\frac{1}{\mu + 2}, \quad (25)$$
$$w_2'(x) = -w_2(x), w_2(0) = 1,$$

where the exact solution is $w_1(x) = -\frac{\exp(-2x)}{\mu+2}$, $w_2(x) = \exp(-x)$ over the interval $[0, 4]$ with $\mu = -10^2$.

The numerical simulations are performed for Problem 2 under the variable stepsize approach setting the tolerance to 10^{-3} and 10^{-4}. Several methods, as mentioned before, are used to compute different types of errors and the number of FEs. For example, it is observed in Table 3 that the block method and its reformulated version used 65 evaluations to yield the errors with 10^{-9}, including OBM with a slightly more significant error. On the other hand, the RK version of the block method under consideration used 108 evaluations but reduced the amount of error to 10^{-10}. The rest of the methods, though performed well enough excluding Radau-I, took more evaluations to yield the errors with 10^{-9} and 10^{-10}. A similar sort of behavior is analyzed in Table 4 for Problem 2 under the variable stepsize approach when the tolerance was set to 10^{-4}.

Problem 3. The four-dimensional periodic orbit system taken from ref. [32] is considered:

$$w_1'(x) = w_2(x), \quad w_1(0) = 1,$$
$$w_2'(x) = -w_1(x) + \frac{\cos(x)}{1,000}, \quad w_2(0) = 0$$
$$w_3'(x) = w_4(x), \quad w_3(0) = 0, \quad (26)$$
$$w_4'(x) = -w_3(x) + \frac{\sin(x)}{1,000}, \quad w_4(0) = \frac{9,995}{10,000},$$

where the exact solution over the interval $[0, 10]$ is given as follows:

$$w_1(x) = \cos(x) + \frac{x \sin(x)}{2,000},$$
$$w_2(x) = \frac{x \cos(x) - 1999 \sin(x)}{2,000},$$
$$w_3(x) = \sin(x) - \frac{x \cos(x)}{2,000}, \quad (27)$$
$$w_4(x) = \frac{x \sin(x) + 1,999 \cos(x)}{2,000}.$$

Table 3: Numerical results for Problem 2 with variable stepsize approach taking the tolerance = 10^{-3}

Method	Norm$_\infty$	RMSE	Mean	FE
Block	1.1102×10^{-9}	7.8513×10^{-10}	5.6469×10^{-10}	65
RBlock	1.1102×10^{-9}	7.8513×10^{-10}	5.6469×10^{-10}	65
RKBlock	3.8194×10^{-10}	2.7007×10^{-10}	1.9106×10^{-10}	108
OBM	3.6797×10^{-9}	2.602×10^{-9}	1.8583×10^{-9}	65
LPHBM	1.4074×10^{-10}	9.9517×10^{-11}	7.0502×10^{-11}	135
Radau-I	1.131×10^{-5}	7.9972×10^{-6}	5.6549×10^{-6}	252
Lob-IIIA	2.2828×10^{-9}	1.6142×10^{-9}	1.1416×10^{-9}	90

Table 2: Comparison of errors with both fixed and variable stepsize approaches for Problem 1, with $\Delta x_{ini} = 10^{-1}$ and $\varepsilon = 10^{-6}$ via two-step optimized block method in (13)

N	FE	Approach	Norm$_\infty$	RMS	Mean
112	1,060	Fixed	5.395×10^{-9}	5.395×10^{-9}	5.395×10^{-9}
112	1,060	Variable	5.551×10^{-17}	3.926×10^{-17}	2.819×10^{-17}

Table 4: Numerical results for Problem 2 with variable stepsize Δx taking the tolerance $= 10^{-4}$

Method	Norm $_\infty$	RMSE	Mean	FE
Block	2.4937×10^{-11}	1.7633×10^{-11}	1.2476×10^{-11}	125
RBlock	2.4937×10^{-11}	1.7633×10^{-11}	1.2476×10^{-11}	125
RKBlock	5.7201×10^{-12}	4.0448×10^{-12}	2.8709×10^{-12}	204
OBM	8.2985×10^{-11}	5.8679×10^{-11}	4.1516×10^{-11}	125
LPHBM	3.9616×10^{-13}	2.8013×10^{-13}	1.9904×10^{-13}	360
Radau-I	1.8982×10^{-7}	1.3422×10^{-7}	9.4917×10^{-8}	260
Lob-IIIA	3.4286×10^{-11}	2.4245×10^{-11}	1.7296×10^{-11}	170

Table 5: Numerical results for Problem 3 with variable stepsize Δx taking the tolerance $= 10^{-1}$

Method	Norm $_\infty$	RMSE	Mean	FE
Block	1.622×10^{-5}	1.365×10^{-5}	1.334×10^{-5}	55
RBlock	1.622×10^{-5}	1.365×10^{-5}	1.334×10^{-5}	55
RKBlock	4.105×10^{-6}	3.453×10^{-6}	3.376×10^{-6}	84
OBM	5.526×10^{-5}	4.65×10^{-5}	4.545×10^{-5}	55
Cheby	1.212×10^{-9}	1.019×10^{-9}	9.965×10^{-10}	295
Radau-I	4.569×10^{-4}	3.555×10^{-4}	3.334×10^{-4}	56
Lob-IIIA	2.497×10^{-5}	2.101×10^{-5}	2.054×10^{-5}	70

Table 6: Numerical results for Problem 3 with variable stepsize h taking the tolerance $= 10^{-3}$

Method	Norm $_\infty$	RMSE	Mean	FE
Block	1.743×10^{-9}	1.466×10^{-9}	1.433×10^{-9}	230
RBlock	1.743×10^{-9}	1.466×10^{-9}	1.433×10^{-9}	230
RKBlock	4.612×10^{-10}	3.88×10^{-10}	3.793×10^{-10}	342
OBM	5.815×10^{-9}	4.892×10^{-9}	4.782×10^{-9}	230
LPHBM	3.553×10^{-14}	2.982×10^{-14}	2.914×10^{-14}	26320
Radau-I	2.197×10^{-7}	1.813×10^{-7}	1.76×10^{-7}	228
Lob-IIIA	2.771×10^{-9}	2.331×10^{-9}	2.279×10^{-9}	285

The numerical simulations are performed for Problem 3 under the variable stepsize approach setting the tolerance to 10^{-1} and 10^{-3}. Several methods, as mentioned before, are used to compute different types of errors and the number of FEs. For example, it is observed in Table 5 that the block method and its reformulated version used 55 evaluations to yield the errors with 10^{-5}, including OBM with a slightly more significant error. On the other hand, the RK version of the block method under consideration used 84 evaluations but reduced the amount of error to 10^{-6}. The rest of the methods, though performed well enough, yielded the errors with 10^{-5} and 10^{-9}. A minor error with 10^{-9} is produced by the sixth-order Cheby; however, the method has used a maximum number of FEs. A similar sort of behavior is analyzed in Table 6 for Problem 3 under the variable stepsize approach when the tolerance was set to 10^{-3}.

Problem 4. The Prothero–Robinson problem [33]:

$$w'(x) = \mu[w(x) - \sin(x)] + s'(x), w(0) = 0, \tag{28}$$
$$x \in [0, 10],$$

where $\mu = 10^{-7}$ and $s(x) = \sin(x)$. The exact solution is $w(x) = \sin(x)$.

The numerical simulations are performed for the Prothero–Robinson problem given in Problem 4 under the variable stepsize approach setting the tolerance to 10^{-2}, 10^{-3}, and 10^{-4}. Table 7 computationally confirms the sixth-order of convergence of (13), since a drop of six orders of magnitude in the maximum absolute error is observed when the number of steps was increased by 1 in the power of 10. Several methods, as mentioned before, are used to compute different types of errors and the

Table 7: A drop of maximum six orders of magnitude in the maximum absolute error for every one rise of magnitude in the number of steps (N) for Problem 4

N	Block	RBlock	RKBlock	OBM	LPHBM	Radau-I	Lob-IIIA
10	2.81×10^{-7}	2.81×10^{-7}	2.81×10^{-7}	9.41×10^{-7}	1.38×10^{-4}	2.85×10^{-5}	6.77×10^{-7}
10^2	2.76×10^{-13}	2.76×10^{-13}	2.76×10^{-13}	9.19×10^{-13}	1.41×10^{-10}	2.78×10^{-10}	6.62×10^{-13}
10^3	2.76×10^{-19}	2.76×10^{-19}	2.76×10^{-19}	9.19×10^{-19}	1.41×10^{-16}	2.78×10^{-15}	6.61×10^{-19}

Table 8: Numerical results for Problem 4 with variable stepsize Δx taking the tolerance $= 10^{-2}$

Method	MaxErr	LastErr	Norm	RMSE	FE
Block	6.493×10^{-9}	3.227×10^{-9}	1.363×10^{-8}	2.905×10^{-9}	105
RBlock	6.493×10^{-9}	3.227×10^{-9}	1.363×10^{-8}	2.905×10^{-9}	105
RKBlock	6.493×10^{-9}	3.227×10^{-9}	1.363×10^{-8}	2.905×10^{-9}	126
OBM	2.166×10^{-8}	1.077×10^{-8}	4.547×10^{-8}	9.693×10^{-9}	105
LPHBM	3.173×10^{-9}	5.029×10^{-10}	9.512×10^{-9}	9.972×10^{-10}	225
Radau-I	1.69×10^{-6}	1.466×10^{-6}	5.051×10^{-6}	1.077×10^{-6}	84
Lob-IIIA	1.559×10^{-8}	7.75×10^{-9}	3.273×10^{-8}	6.978×10^{-9}	105

Table 9: Numerical results for Problem 4 with variable stepsize Δx taking the tolerance $= 10^{-3}$

Method	MaxErr	LastErr	Norm	RMSE	FE
Block	5.167×10^{-11}	4.395×10^{-11}	1.807×10^{-10}	2.756×10^{-11}	210
RBlock	5.167×10^{-11}	4.395×10^{-11}	1.807×10^{-10}	2.756×10^{-11}	210
RKBlock	5.167×10^{-11}	4.395×10^{-11}	1.807×10^{-10}	2.756×10^{-11}	252
OBM	1.723×10^{-10}	1.465×10^{-10}	6.025×10^{-10}	9.187×10^{-11}	210
LPHBM	1.490×10^{-11}	2.066×10^{-12}	7.92×10^{-11}	4.865×10^{-12}	660
Radau-I	5.133×10^{-8}	5.046×10^{-8}	1.946×10^{-7}	2.967×10^{-8}	168
Lob-IIIA	1.24×10^{-10}	1.055×10^{-10}	4.337×10^{-10}	6.615×10^{-11}	210

Table 10: Numerical results for Problem 4 with variable stepsize Δx taking the tolerance $= 10^{-4}$

Method	MaxErr	LastErr	Norm	RMSE	FE
Block	7.505×10^{-13}	2.237×10^{-13}	3.063×10^{-12}	3.265×10^{-13}	435
RBlock	7.518×10^{-13}	2.202×10^{-13}	3.067×10^{-12}	3.269×10^{-13}	435
RKBlock	7.493×10^{-13}	2.266×10^{-13}	3.062×10^{-12}	3.265×10^{-13}	522
OBM	2.502×10^{-12}	7.517×10^{-13}	1.021×10^{-11}	1.089×10^{-12}	435
LPHBM	6.181×10^{-14}	3.431×10^{-14}	8.979×10^{-13}	3.141×10^{-14}	2040
Radau-I	1.381×10^{-9}	9.632×10^{-10}	8.089×10^{-9}	8.623×10^{-10}	348
Lob-IIIA	1.802×10^{-12}	5.406×10^{-13}	7.354×10^{-12}	7.84×10^{-13}	435

number of FEs. For example, it is observed in Table 8 for the tolerance to 10^{-2} that the block method and its reformulated version used 105 evaluations to yield the errors with 10^{-9}, including OBM and Lob-IIIA methods with a slightly more significant error. On the other hand, the RK version of the block method under consideration used 126 evaluations; however, the errors are the same as in the previous two cases. One of the reasons could be the stiff nature of the problem under consideration. The smallest error with 10^{-9} is produced by the sixth-order LPHBM;

Table 11: A drop of maximum six orders of magnitude in the maximum absolute error for every one rise of magnitude in the number of steps (N) in Problem 5

N	Block	RBlock	RKBlock	OBM	LPHBM	Radau-I	Lob-IIIA
10	1.71×10^{-1}	1.71×10^{-1}	1.71×10^{-1}	2.30×10^{-1}	4.37×10^{-1}	4.33×10^{4}	3.03×10^{-1}
10^2	3.59×10^{-5}	3.59×10^{-5}	3.59×10^{-5}	1.11×10^{-4}	1.86×10^{-3}	2.00×10^{-3}	2.00×10^{-4}
10^3	3.90×10^{-11}	3.90×10^{-11}	3.90×10^{-11}	1.30×10^{-10}	7.21×10^{-9}	1.70×10^{-8}	2.34×10^{-10}

Table 12: Numerical results for Problem 5 with variable stepsize Δx taking the tolerance $= 10^{-2}$

Method	MaxErr	LastErr	Norm	RMSE	FE
Block	5.138×10^{-7}	5.891×10^{-8}	7.787×10^{-7}	2.081×10^{-7}	65
RBlock	5.138×10^{-7}	5.891×10^{-8}	7.787×10^{-7}	2.081×10^{-7}	65
RKBlock	1.329×10^{-7}	8.782×10^{-14}	1.968×10^{-7}	3.655×10^{-8}	168
OBM	1.315×10^{-6}	1.635×10^{-7}	1.961×10^{-6}	5.24×10^{-7}	65
LPHBM	5.899×10^{-7}	4.338×10^{-10}	7.859×10^{-7}	1.172×10^{-7}	110
Radau-I	5.39×10^{-6}	1.169×10^{-6}	1.008×10^{-5}	1.871×10^{-6}	112
Lob-IIIA	6.343×10^{-7}	3.267×10^{-11}	9.64×10^{-7}	1.79×10^{-7}	140

Table 13: Numerical results for Problem 5 with variable stepsize Δx taking the tolerance $= 10^{-3}$

Method	MaxErr	LastErr	Norm	RMSE	FE
Block	5.555×10^{-8}	1.8×10^{-10}	7.545×10^{-8}	1.573×10^{-8}	110
RBlock	5.555×10^{-8}	1.8×10^{-10}	7.545×10^{-8}	1.573×10^{-8}	110
RKBlock	1.029×10^{-8}	2.22×10^{-16}	1.423×10^{-8}	1.885×10^{-9}	336
OBM	1.447×10^{-7}	1.192×10^{-9}	1.932×10^{-7}	4.028×10^{-8}	110
LPHBM	3.55×10^{-8}	9.537×10^{-14}	5.09×10^{-8}	4.788×10^{-9}	280
Radau-I	4.435×10^{-7}	7.083×10^{-11}	8.041×10^{-7}	1.065×10^{-7}	224
Lob-IIIA	5.371×10^{-8}	1.315×10^{-13}	7.609×10^{-8}	1.008×10^{-8}	280

however, the method has used a maximum number of FEs. A similar sort of behavior is analyzed in Tables 9 and 10 for Problem 3 under the variable stepsize approach when the tolerance was set to 10^{-3} and 10^{-4}, respectively.

Problem 5. The highly oscillatory problem [34]:

$$w'(x) = -\sin(x) - 200[w(x) - \cos(x)],$$
$$w(0) = 0, \quad x \in [0, 1], \tag{29}$$

where the exact solution is $w(x) = \cos(x) - \exp(-200x)$.

The numerical simulations are performed for the highly oscillatory problem given in Problem 5 under the variable stepsize approach setting the tolerance to 10^{-2}, 10^{-3}, and 10^{-4}. Table 11 computationally confirms the

sixth-order of convergence of (13), since a drop of six orders of magnitude in the maximum absolute error is observed when the number of steps was increased by 1 in the power of 10, though this pattern starts to appear after 10^2 steps. Several methods, as mentioned before, are used to compute different types of errors and the number of FEs. For example, it is observed in Table 12 for the tolerance to 10^{-2} that the block method and its reformulated version used 65 evaluations to yield the errors with 10^{-7}, including OBM with a slightly more significant error. On the other hand, the RK version of the block method under consideration used 168 evaluations but reduced the amount of maximum absolute error to 1.329×10^{-7} and the smallest absolute error at the last grid point of the integration interval [0, 1]. The other methods have

Table 14: Numerical results for Problem 5 with variable stepsize Δx taking the tolerance $= 10^{-4}$

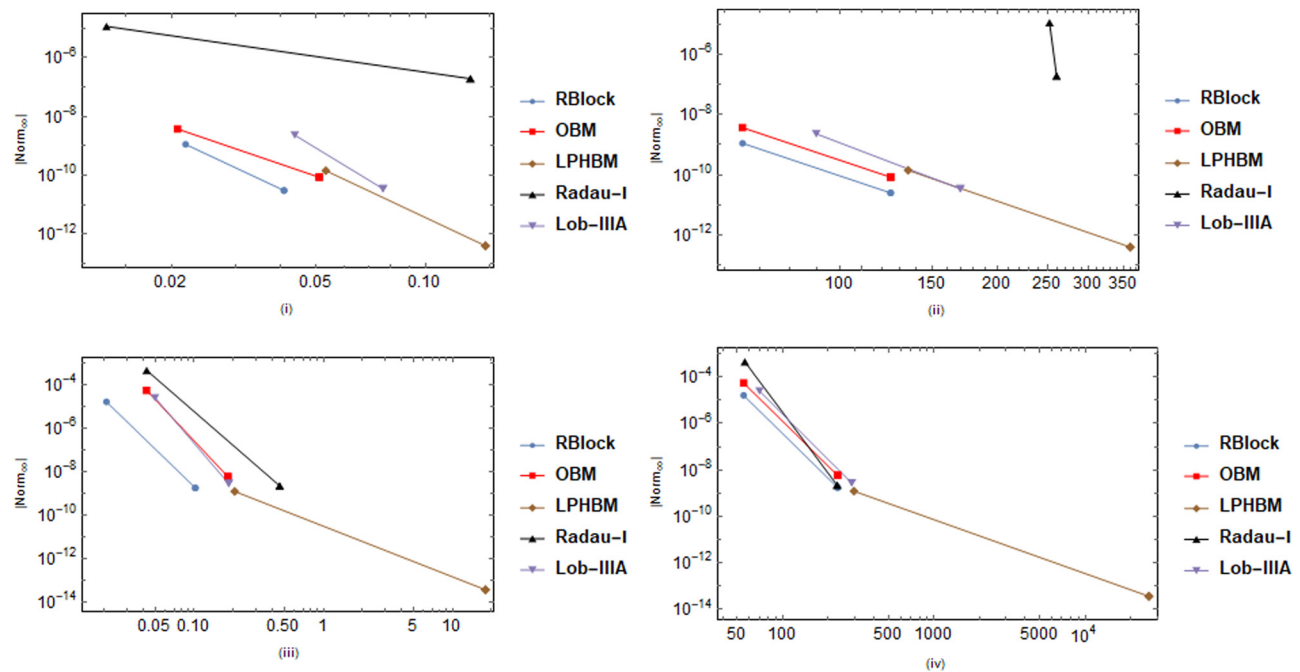| Method	MaxErr	LastErr	Norm	RMSE	FE
Block	5.732×10^{-9}	5.884×10^{-14}	7.538×10^{-9}	1.15×10^{-9}	210
RBlock	5.732×10^{-9}	5.873×10^{-14}	7.538×10^{-9}	1.15×10^{-9}	210
RKBlock	4.214×10^{-10}	0	6.737×10^{-10}	6.255×10^{-11}	690
OBM	1.288×10^{-8}	2.748×10^{-13}	1.93×10^{-8}	2.942×10^{-9}	210
LPHBM	1.051×10^{-9}	3.331×10^{-16}	1.474×10^{-9}	8.152×10^{-11}	815
Radau-I	2.883×10^{-8}	1.581×10^{-11}	5.598×10^{-8}	5.197×10^{-9}	460
Lob-IIIA	2.413×10^{-9}	1.732×10^{-14}	3.873×10^{-9}	3.596×10^{-10}	575

Figure 3: Comparison of the efficiency curves for Problems 2 (top two) and 3 (bottom two) under consideration while taking variable step-size formulation for each method.

used more FEs to yield a comparable amount of error. A similar sort of behavior is analyzed in Tables 13 and 14 for Problem 5 under the variable stepsize approach when the tolerance was set to 10^{-3} and 10^{-4}, respectively.

5.1 Efficiency curves with variable stepsize

In this section, we present some efficiency curves for the differential systems taken into consideration.
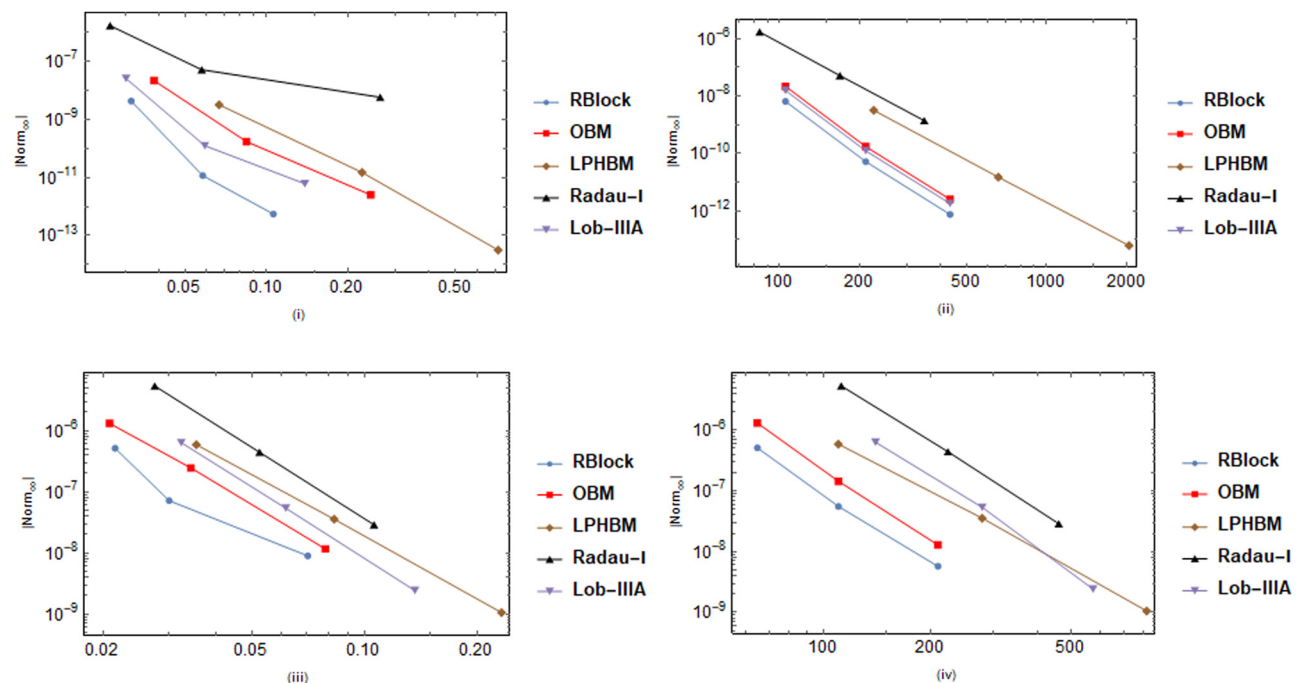
Figure 4: Comparison of the efficiency curves for Problems 4 (top two) and 5 (bottom two) under consideration while taking variable step-size formulation for each method.

The presentation of the efficiency curves is a very useful way to compare the performance of different methods and is commonly used in numerical analysis articles. It allows us to quickly see which methods work best. Figures 3 and 4 represent the comparison of the efficiency curves for each method under consideration, excluding the block and its RK version, for its reformulation already saves the computational cost. The comparison is based on absolute maximum global error (Norm) versus CPU time and the absolute maximum global error versus the number of FEs. It may be noted that these curves are obtained with variable stepsize formulation for the reformulated version of the two-step optimized block method as given in (14). The performance of Problems 2 and 3 is shown by plots (i), (ii), (iii), and (iv) in Figure 3, while performance of Problems 4 and 5 is shown by plots (i), (ii), (iii), and (iv) in Figure 4. Each plot shows that the reformulated version of the two-step optimized block method (RBlock) is computationally inexpensive compared to other methods in the context of the CPU time (seconds) and the number of FEs.

6 Conclusion and future plan

In this research, a variable stepsize is mainly focused on a two-step optimized block method, including its relative stability. The motivation of the present work is based on recently published research by Ramos [18], wherein only a fixed stepsize approach was discussed along with linear stability, zero-stability, consistency, and convergence analysis. We have presented the method afresh, including its reformulated version and RK form, for solving the differential systems emerging from several areas of scientific study. The main focus of the present research analysis is the variable stepsize approach that shows superiority over several existing block types and classical families of implicit methods when tested on stiff and nonlinear differential systems occurring in many applications. Furthermore, the relative stability analysis of order stars is discussed in detail. The variable stepsize version of the presented block method is applicable for solving many physical systems that arise in the fields of science and engineering.

We intend to develop a new family of OBMs with $\mathcal{L}$-stability in the future. Moreover, we have also planned to extend our current research work toward the solution of delay differential equations, fractional differential equations, and partial differential equations as done in refs [35–39] and in some of the works cited therein.

References

[1] Musa SS, Qureshi S, Zhao S, Yusuf A, Mustapha UT, He D. Mathematical modeling of COVID-19 epidemic with effect of awareness programs. Infectious Disease Modelling. 2021 Jan 1;6:448–60.

[2] Memon Z, Qureshi S, Memon BR. Assessing the role of quarantine and isolation as control strategies for COVID-19 outbreak: a case study. Chaos Solitons Fractals. 2021 Mar 1;144:110655.

[3] Peter OJ, Qureshi S, Yusuf A, Al-Shomrani M, Idowu AA. A new mathematical model of COVID-19 using real data from Pakistan. Results Phys. 2021 May 1;24:104098.

[4] Wang RS. Ordinary differential equation (ODE), model encyclopedia of systems biology. Dubitzky W, Wolkenhauer O, Cho KH, Yokota H, eds. New York, NY: Springer; 2013. p. 1606–8.

[5] Zill DG. Differential equations with boundary-value problems. Cengage learning. USA: Cengage; 2016 Dec 5.

[6] Urasaki S, Yabuno H. Identification method for backbone curve of cantilever beam using van der Pol-type self-excited oscillation. Nonlinear Dynamics. 2021 Mar;103(4):3429–42.

[7] Ahmad I, Raja MAZ, Ramos H, Bilal M, Shoaib M. Integrated neuro-evolution-based computing solver for dynamics of nonlinear corneal shape model numerically. Neural Comput Appl. 2021;33(11):5753–69.

[8] Zill DG. A first course in differential equations with modeling applications. Cengage learning. USA: Cengage; 2012 Mar 15.

[9] Zill DG. Advanced engineering mathematics. USA: Jones & Bartlett Publishers; 2020 Nov 20.

[10] Qureshi S, Yusuf A, Aziz S. Fractional numerical dynamics for the logistic population growth model under Conformable Caputo: a case study with real observations. Phys Scr 2021;96(11):114002.

[11] Rufai MA, Ramos H. One-step hybrid block method containing third derivatives and improving strategies for solving Bratu's and Troesch's problems. Numer Math Theory Methods Appl. 2020;13(4):946–72.

[12] Singh G, Garg A, Kanwar V, Ramos H. An efficient optimized adaptive step-size hybrid block method for integrating differential systems. Appl Math Comput. 2019 Dec 1;362:124567.

[13] Ramos H, Jator SN, Modebei MI. Efficient k-step linear block methods to solve second order initial value problems directly. Mathematics. 2020 Oct 12;8(10):1752.

[14] Ramos H, Abdulganiy R, Olowe R, Jator S. A family of functionally-fitted third derivative block Falkner methods for solving second-order initial-value problems with oscillating solutions. Mathematics. 2021 Mar 25;9(7):713.

[15] Olagunju A, Adeyefa E. Hybrid block method for direct integration of first, second and third order IVPs. Cankaya Univ J Sci Eng. 2021;18(1):1–8.

[16] Ramos H, Qureshi S, Soomro A. Adaptive step-size approach for Simpson's-type block methods with time efficiency and order stars. Comput Appl Math. 2021 Sep;40(6):1–20.

[17] Kashkari BS, Alqarni S. Optimization of two-step block method with three hybrid points for solving third order initial value problems. J Nonlinear Sci Appl. 2019 Mar;12:450.

[18] Ramos H. Development of a new Runge-Kutta method and its economical implementation. Comput Math Meth. 2019 Mar;1(2):e1016.

[19] Ramos H, Singh G. A note on variable step-size formulation of a Simpson's-type second derivative block method for solving stiff systems. Appl Math Lett. 2017 Feb 1;64:101–7.

[20] Ramos H, Kalogiratou Z, Monovasilis T, Simos TE. An optimized two-step hybrid block method for solving general second order initial-value problems. Numer Algorithms. 2016 Aug;72(4):1089–102.

[21] Sofroniou M. Order stars and linear stability theory. J Symbolic Comput. 1996 Jan 1;21(1):101–31.

[22] Wolfram S. Mathematica® 3.0 Standard Add-on Packages. USA: Cambridge University Press; 1996 Sep 13.

[23] Iserles A, Norsett SP. Order stars: theory and applications. Britain: CRC Press; 1991 Jun 1.

[24] Shampine LF. Computer solution of ordinary differential equations. The initial value problem. Jordan: WH Freeman; 1975.

[25] Hairer P. Solving ordinary differential equations II. Berlin Heidelberg: Springer; 1991.

[26] Watts HA. Starting step size for an ODE solver. J Comput Appl Math. 1983 Jun 1;9(2):177–91.

[27] Sedgwick AE. An effective variable-order variable-step adams method. PhD thesis, University of Toronto, 1973.

[28] Sunday J, Kolawole FM, Ibijola EA, Ogunrinde RB. Two-step Laguerre polynomial hybrid block method for stiff and oscillatory first-order ordinary differential equations. J Math Comput Sci. 2015 Sep 26;5(5):658–68.

[29] Butcher JC. Numerical methods for ordinary differential equations. New Zealand: John Wiley & Sons; 2016 Aug 29.

[30] Qureshi S, Soomro A, Hinçal E. A new family of $\mathcal{A}$-acceptable nonlinear methods with fixed and variable stepsize approach. Comput Math Meth. 2021 Nov;3(6):e1213.

[31] Khalsaraei MM, Oskuyi NN, Hojjati G. A class of second derivative multistep methods for stiff systems. Acta Universitatis Apulensis. 2012;30:171–88.

[32] Stiefel E, Bettis DG. Stabilization of Cowell's method. Numerische Mathematik. 1969 May;13(2):154–75.

[33] Prothero A, Robinson A. On the stability and accuracy of one-step methods for solving stiff systems of ordinary differential equations. Math Comput. 1974;28(125):145–62.

[34] Abdulganiy RI, Akinfenwa OA, Okunuga SA. Construction of L stable second derivative trigonometrically fitted block backward differentiation formula for the solution of oscillatory initial value problems. African J Sci Technol Innovat Development. 2018 Jul 1;10(4):411–9.

[35] Senu N, Lee KC, Ahmadian A, Ibrahim SN. Numerical solution of delay differential equation using two-derivative Runge-Kutta type method with Newton interpolation. Alexandr Eng J. 2022 Aug 1;61(8):5819–35.

[36] Darehmiraki M, Rezazadeh A, Ahmadian A, Salahshour S. An interpolation method for the optimal control problem governed by the elliptic convection-diffusion equation. Numer Meth Partial Differ Equ. 2022 Mar;38(2):137–59.

[37] Lee KC, Senu N, Ahmadian A, Ibrahim SN. On two-derivative Runge-Kutta type methods for solving $u = f(x, u(x))$ with application to thin film flow problem. Symmetry. 2020 Jun;12(6):924.

[38] Khader MM, Saad KM, Baleanu D, Kumar S. A spectral collocation method for fractional chemical clock reactions. Comput Appl Math. 2020 Dec;39(4):1–2.

[39] Alomari AK, Abdeljawad T, Baleanu D, Saad KM, Al-Mdallal QM. Numerical solutions of fractional parabolic equations with generalized Mittag-Leffler kernels. Numer Meth Partial Differ Equ. 2020:1–13. https://doi.org/10.1002/num.22699.

Appendix

Algorithm 1: Pseudo-code for the two-step optimized hybrid block method with two intra-step points under fixed stepsize approach

---

    Data: a, b (integration interval), N (number of steps), w_{00}, w_{10}, (initial values), g

    Result: sol (discrete approximate solution of the IVP (1))

1   Let $n = 0$, $\Delta x = \frac{b-a}{N}$

2   Let $x_n = x_0$, $w_n = w_{00}$, $w'_n = w'_{10}$

3   Let **sol** $= \{(x_n, w_n)\}$

4   Solve (13) to obtain w_{n+k}, w'_{n+k}, where $k = 0, r, 1, s, 2$

5   Let **sol** = **sol** $\cup \{(x_{n+k}, w_{n+k})\}_{k=0,r,1,s,2}$

6   Let $x_n = x_n + 2\Delta x$, $w_n = w_{n+2}$, $w'_n = w'_{n+2}$

7   Let $n = n + 2$

8   **if** $n = N$ **then**

9 | go to 13

10   **else**

11 | go to 4;

12   **end**

13   End

Algorithm 2: Pseudo-code for the two-step optimized hybrid block method with two intra-step points under variable stepsize approach

---

    Data: Initial stepsize: $\Delta x = \Delta x_0 = \Delta x_{\text{old}}$, $x_m := x_0$, $w_m := w_0$; Integration interval: $[x_0, b]$; Initial value: w_0; Function g: $g(x, w(x))$; Given tolerance: TOL

1   **Result**: Approximations of problem (1) at selected points.

2   **if** $x_m \geq b$ **then**

3   **end**

4   **if** $x_m + \Delta x > b$, $\Delta x = b - x_0$ **then**

5   **end**

6   **while** $x_m < b$, then solve system of equations in (13) to get the values w_{n+1} **do**

7 | compute w^*_{n+1} to get EST.

8   **end**

9   **if** $|\text{EST}| \leq \text{TOL}$ then accept the results and substitute $\Delta x_{\text{new}} = 2 \times \Delta x_{\text{old}}$ **then**

10   **end**

11   Set $x_n = x_n + 2\Delta x$, $n = n + 2$ and use the formula in (21) to determine the new stepsize.

12   **if** $|\text{EST}| > \text{TOL}$, then reject the results and repeat the calculations using (21) and go to step (6) **then**

13   **end**

14   end